IRACST – Engineering Science and Technology: An International Journal (ESTIJ), ISSN: 2250-3498, Vol.3, No.4,August 2013

Case Study of Full Field Simulation Faulted Anticline Reservoir

Mohamed .A.Elhemry[1,*], Kulud.M.Rhumua[1]
[1]*Petroleum Eng. Dept., University of Tripoli,*
Tripoli , Libya

Ibrahim Musbah[3], Rahil.O.Abdulhadi[4]
[3]*Petroleum Eng. Dept., University of Sirte,*
[4] *Mechanical Eng. Dept., University of Sebha,*
Sirte and Sebha, Libya

Abstract **- A recent simulation study was conducted on a faulted anticlined reservoir located in exploration area NC177, in En Naga sub of the Sirte basin. The field contained three types of formations, Beda, Zelten and Gir formation. The aim this study is to update the dynamic model of the reservoir with a new data available. The new currently available data including gas, oil and water production history, injection history including daily and monthly injection rate of each injector well in the reservoir. Also well coordinates and perforation interval and location of the infill wells , the model become an effective and rapid predictive tool and was used to evalute numerous development scenarios in a relatively short space and time. Static and dynamic model of the reservoir were examined and data were prepared for history matching, prediction and recommendation for further developlment. Those was done through different steps including studying the geological survey, modifying , 3D geological model using Peterl, and updating and running simulation study with different possible cases of dynamic models usinf Eclipse.**

Keywords-component; En Naga, Beda formation; Zelten formation; Gir formation; Simulation

I. INTRODUCTION

En Naga field is situated in exploitation area NC177, in the En Naga Sub basin of the Sirte basin, about 150 km southwest of Tibisti field, 200 km south of Ras Lanuf [1]. This field is Harougu's latest development and went on production in 2003. The filed was discovered by Lundin, who assigned its right and obligations to petro-Canda in 2002. The geological strike, from En Naga dicoveries in concession 72 [2]. details on the geological structural of Sirte basin can be found in [3,4]. The full-field dynamic simulation model represents the culmination of Phase II Field Development Plan (FDP), which Studies a reservoir engineering work program. It combines all the elements described in previous sections of this study published [5] into a single tool for analyzing and predicting future performance of the En Naga reservoirs. Once calibrated to known field data, the model is becoming an effective and rapid predictive tool that can be used to evaluate numerous development scenarios in relatively short space and time. The impact of new wells, revised operating constraints, and secondary recovery techniques on future production can all be accurately assessed. The En Naga simulation model therefore has been used as the basis for evaluation of the various scenarios: its production forecasts the corresponding expenditure and being subject to economic analysis in order to select the final option. Since the four reservoirs of the En Naga field are isolated and their subsurface operating constraints largely independent, new model has been designed to be run either as an integrated full-field model, or as four separate models. This allows a greater degree of flexibility when, for example, examining different combinations of infill drilling patterns. The following sections describe the construction and calibration of the new model.

II. SIMULATION GRIDS CONSTRUCTION

The simulation grid was exported directly from the Petrel 3D geological model, Petrel 3D was used to assemble the overall structure of the grid, defines the vertical layering and zonation scheme, and populates the grid with porosity and water saturation distributions. The location and trajectory of all infield faults were also captured at this stage. This grid was ultimately up-scaled to a roughly orthogonal pattern, conforming to the major fault orientations, giving an average cell size of approximately 100m x 100m. For simulation purposes, the original scheme of 149 layers was up-scaled to 46 layers in Petrel, covering the entire En Naga section from Top Gir F7 Dolomite through to Base Beda-C. This 46 layer scheme still included some non-reservoir layers, such as the intervening anhydrites in the Gir section. To reduce the size of the simulation input datasets, and make the final simulation model less cumbersome, these non-reservoir units were removed, reducing layers count further to just 28 layers. This editing of the Petrel grid data was performed outside of Petrel by manually deleting the co-ordinate and property data for the appropriate layers in the exported ASCII grid files. Note that this process does not constitute further up-scaling and it did not adversely impact the vertical resolution of the reservoir description: these were non-reservoir units being removed, the hydrocarbon-bearing layers being maintained intact. Table **I** illustrates the final 28 layer system used in the simulation model, and correlates the Eclipse simulation layers back to the original Petrel geological model layers and surfaces. The layering scheme can be broken down into three reservoirs each one contains different amounts of layers as show in below.

Table I: Geological Model vs. Simulation Model Layers

Formation	Geological Model	Simulation Model
Basal Gir	25 layers	15 layers
Zelten -A	6 layers	5 layers
Beda- C	15 layers	8 layers
Total	46 layers	28 layers

The resulting simulation grid had a total of 544,040 cells: 134 in the X-direction, 145 in the Y-direction, giving 19,430 cells in each of the 28 layers. Much of the peripheral grid area lay outside the field limits and could be de-activated before proceeding with simulation. By removing these outlying areas from the model the total cell count was reduced by 35%, leaving an "active" cell count of only 352,409. **Fig.1** gives an overall 3D view of the integrated simulation grid, while **Fig.2** offers a close up view of the Gir section, clearly showing the "gaps" left by the removal of the non-reservoir anhydrite layers.

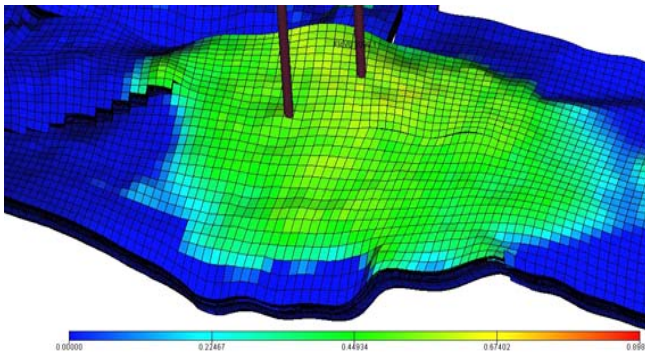

Fig.1: Overall 3D view of the simulation grid

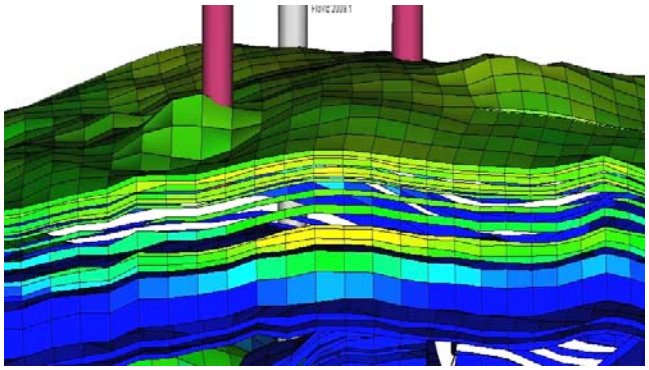

Fig.2: A close up view of the Gir west layers.

III. Rock and Fluid Properties

A. Porosity and Water Saturation

The porosity and water saturation distributions were exported from Petrel and incorporated into the Eclipse simulation grid with no further modification as shown in **Fig.3**. It is important to mention that the water saturation distribution was carried over from Petrel model intact, and effectively "hard-coded" into the Eclipse input data **Fig.4**. This is not the conventional method for setting up the initial saturation distribution in a simulation model: normally this is achieved through the use of capillary pressure curves which express pc as a function of water saturation, Sw. The dependence of pc on porosity is handled in this case by dividing the model grid cells into a number of porosity "classes" and assigning a separate curve for each. With this method it can be difficult to match exactly the saturation distribution and hence (STOIIP) generated by the original Sw-h function. These difficulties arise when using a number of porosity classes inevitably introduces an element of approximation, since each class covers a range of porosity values, whereas the original Sw-h function includes φ in its formulation; also a single average value for density difference, Δρ, has to be chosen to convert from Sw-h to pc, moreover the simulator will calculate Δρ with depth to convert back.

This is avoided by invoking Eclipse's "End-Point Scaling" option in the initialization. This option effectively reads the input initial water saturation array and "scales" any input capillary pressure curves to honor the input saturation in each cell. In this way the water saturation array computed and upscaled in Petrel is exactly matched in the Eclipse simulation model without any further manipulation. It also ensures that the results of the volumetric calculations in the two model types are almost identical, any difference in surface volumes being attributable solely to the averaging of the formation volume factor. Zonal averages for porosity and water saturation taken from the hydrocarbon-bearing areas of the simulation model are tabulated below: As can be seen from the Table II, much of the Gir reservoir is in the transition zone and hence average water saturations are relatively high.

Table II: Zonal averages for porosity and water saturation

Reservoir	Zone	*φavg*	*Swavg*
Gir North	F7	0.200	0.600
	F6	0.246	0.529
	F5	0.214	0.584
	F4	0.188	0.633
	F3	0.210	0.616
	G2	0.261	0.561
	G1	0.128	0.737
Gir West	F7	0.197	0.637
	F6	0.246	0.631
	F5	0.210	0.654
	F4	0.201	0.672
	F3	0.200	0.596
	G2	0.262	0.596
	G1	0.160	0.779

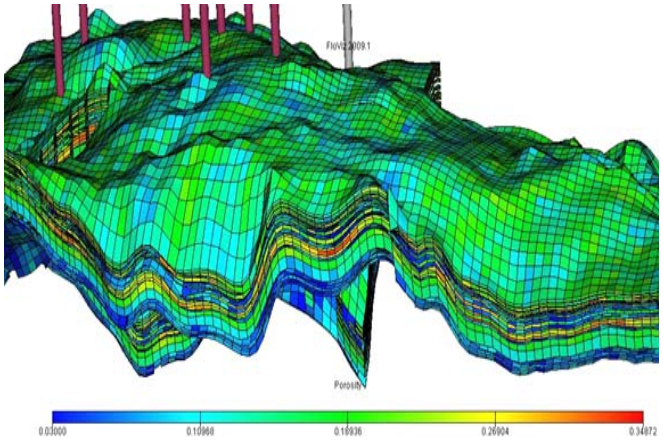

Fig.3: 3D view of the porosity distribution across grid

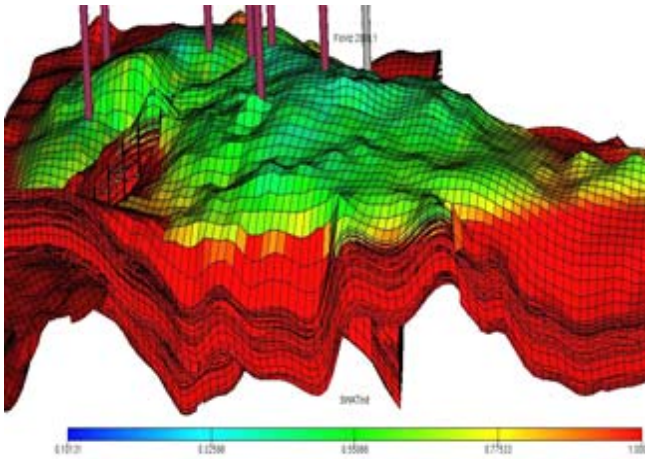

Fig.4: 3D view of the initial water saturation distribution.

B.Permeability

The development of porosity-permeability transforms from the available laboratory core analysis results. Permeability arrays for the simulation grid were generated in the FloGrid pre-processing software by implementing the transforms on a layer-by-layer basis. It should be noted that the resulting permeability distributions were considered a "first pass" since they would have to be later modified during history-matching in order to match actual well performance and, on a layer-by-layer basis, to match observed differential depletion profiles. Using available core data on vertical permeability, the ratio of vertical permeability to horizontal permeability, kv/kh, in the model was initially set to 0.10 in the Gir and Beda-C reservoirs, and 0.50 in the Zelten-A. These ratios were subsequently modified in the history-matching process in order to replicate observed well performance. Explicit zero vertical transmissibility multipliers were put in the model to isolate the Gir dolomite unit from one another, reproducing the effect of the sealing anhydrite layers between them. The exceptions to this are the G2 and G1 dolomites at the base of the Gir sequence which the MDT logging of wells B9 and B10 showed to be in full communication.

C. Saturation-Dependent Function

The evaluation of the recent SCAL data and the generation of water-oil relative Permeability curves for each formation type were explained. No new gas oil relative permeability data were available, so the gas-oil curves were carried over from the previous simulation study. The water-oil tables were generated by simply de-normalizing a generic curve using the appropriate values of Sor, krw(end). Note that the input values of connate water saturation, Swc, and maximum capillary pressure, pc(max), are "dummy"values since these are scaled to honor the input water saturation array according to the Eclipse "End-Point Scaling" algorithm. Additional "straight line" relative permeability curves were assigned to all well connection cells. This was designed to emulate the two-phase flow condition which is believed to occur as fluid enters the wellbore. That is, water and oil rarely enter the wellbore at exactly the same point in practice, so within the resolution of a simulation cell block segregated flow can be said to occur. This flow condition is modeled as simple straight-line relative permeability curves: the effective permeability of one phase essentially being directly proportional to its saturation. Without this modification, the total effectively permeability at the well cells (and hence the PI of the well) is drastically reduced as soon as the water saturation in those cells increases above connate, a phenomenon rarely observed in the field. One problem with the end-point scaling option is that it can leave all water saturations above the oil-water contact immobile, which is unrealistic if a large transition zone exists in which water is mobile. By default, all connate water saturations will be set equal to the input saturation array, and by definition this end-point will be immobile. However, in reality, in the transition zone some of the initial saturations are actually mobile: in other words the critical water saturation, Swcr, is less than the initial water saturation, Swi. To reproduce this effect in the model, a threshold value of water saturation must be determined: if the initial water saturation is below this value (ie high up in the transition zone), then the critical saturation is set equal to the input initial saturation and the water is initially immobile, where if the initial saturation is higher than this value then the critical saturation is set equal to the fixed threshold value and the initial water is mobile. As a result of the history-matching process a suitable value for this threshold water saturation value was found to be 0.70. Expressed mathematically, the algorithm to determine critical water saturation was as follows:

$$\text{If: } (Swi < 0.70) \text{ (Then: } Swcr = Swi) \text{ (Else: } Swcr = 0.70)$$

Another problem arises in the transition zone when the input initial water saturation, Swi, is so high that the mobile saturation range reduces to zero (or becomes negative) such that:

$$1 - Swi - Sor < 0$$

Without any modification to the residual oil saturation, Sor, this will render the fluids completely immobile in the lower part of the transition zone. To get around this problem, Sor was scaled down in regions of high Swi, such that there was always a finite mobile saturation range within the transition zone. An

algorithm was developed such that if a cell's initial water saturation exceeded a certain threshold value, its residual oil saturation was scaled down from its initial value, on a sliding scale down to a minimum of zero at the OWC where (Swi= 1.0) **Fig.5**.

D. Fluid Properties

Oil properties were taken from the PVT report for the appropriate fluid sample, converted to field conditions. The oil formation volume factor, Bo, solution gas/oil ratio, Rs, and oil viscosity, μo, for each fluid type as a function pressure. A full set of gas properties was not available in the PVT reports, so instead correlations were used to generate compressibility factor, Z, and gas viscosity, μg as a function of pressure for each fluid type. These correlations were tuned to the limited laboratory data available by adjusting the input gas gravity in order to match the reported Z-factor at the bubble point. Physical properties of the formation waters were also not generally available at the time of model construction so, again, industry-standard correlations were used to derive the following values, based on the known reservoir pressures and temperatures and approximate water salinities:

Table III: Physical properties of the formation waters

Parameter	Gir North	Gir West
***Bw*(rb/stb)**	1.019	1.018
***cw*(1/psi)**	2.76x10-6	2.75x10-6
μw(cp)	0.429	0.438

IV. REGION ALLOCATION

In a field with multiple reservoirs or regions, such as En Naga, Eclipse requires that each cell of the simulation grid be assigned a number of "region numbers" to allocate the cell to a particular fluid type, saturation function table number, or equilibration region. It is also possible to split the model into different volumetric regions for reporting purposes in order, for example, to track STOIIP and recovery efficiency on a layer-by-layer basis. The following region numbers were therefore assigned to the model:

Table IV: Region Number's

Reservoir	Zone	Volumetric Region	PVT Region	Equilibration Region
Gir North	F7	1	1	1
	F6	2	1	1
	F5	3	1	1
	F4	4	1	1
	F3	5	1	1
	G2	6	1	1
	G1	7	1	1
Gir West	F7	8	2	2
	F6	9	2	2
	F5	10	2	2
	F4	11	2	2
	F3	12	2	2
	G2	13	2	2
	G1	14	2	2

V. EQUILIBRATION AND INITILIZATION

For each of the "equilibration" regions specified in region allocation section, Eclipse requires an initial reservoir pressure at a datum depth in order to initialize the model's pressure and saturation distributions. It also requires the oil-water and gas-oil contact (OWC and GOC) depths for each. The following data was therefore used for the four separate equilibration regions:

Table V: Equilibration regions data

Reservoir	Reservoir Pressure (psia)	Datum Depth (ft TVDSS)	OWC Depth (ft TVDSS)	GOC Depth (ft TVDSS)
Gir North	2,306	4,648	4,750	-
Gir West	2,194	4,337	4,432	-

With the exception of Gir North, all contact depths are based on the structural spill point of each reservoir, as discussed in Petrophysical Data Section. Although PVT sample was not available to confirm, it is believed that the Beda C reservoir was initially in a saturated condition, logs indicating a possible gas-oil contact (GOC) at 7,050 ft TVDSS. All other reservoirs were initially under saturated with no primary gas cap.

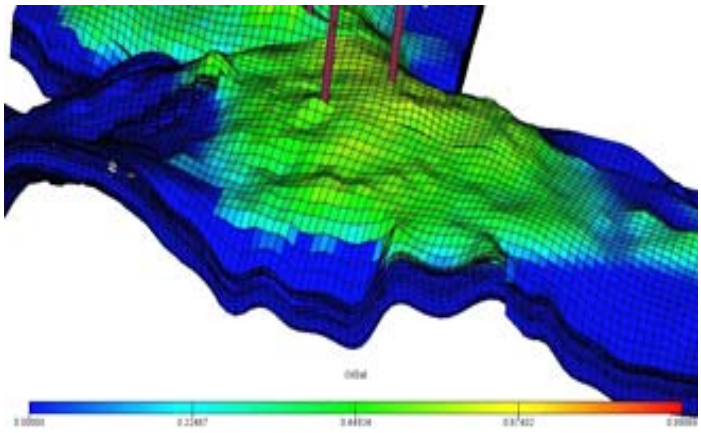

Fig.5: 3D view of the oil saturation distribution.

Eclipse normally uses the contact depth information together with the input capillary pressure curves to establish the initial fluid saturations in each cell of the model. However, since "End-Point Scaling" option was used, any capillary pressure curves are effectively overridden and the model equilibrates to honor the input water saturation array.

Having set up the initial pressures and saturation distributions, the model can then be initialized and volumetrics calculated. The final oil-in-place volumes for each of the equilibration regions were as follows:

Table VI: Oil-in-place for each of the equilibration regions

Reservoir	STOIIP (MMstb)
Gir North	35
Gir West	65

VI. AQUIFER DESCRIPTION

Although simulation grid does cover peripheral areas outside of the main oil accumulations in En Naga, the greater extent of the aquifers in communication with the oil column was represented in the model by Carter-Tracy analytic aquifers. At the Gir level, these aquifers were attached to the north-eastern and south-western sides of the grid to act on the Gir North and Gir West reservoirs respectively, while a single aquifer on the north-eastern edge of the grid influenced the Zelten-A reservoir. Appropriate reservoir properties of porosity, permeability and thickness were assigned to these aquifers. During the history-matching of the model the influence of these analytic aquifers was found to be small and the well responses relatively insensitive to change in aquifer properties. It is believed that this is partially due to the relatively low permeability of the aquifers but, more importantly, due to the relatively small cumulative recovery from the field during its first 1½ to 2 years on production.

Acknowledgment

The authors thank Haroug Oil Operation in Libya for their support and provided us with the necessary information needed for this study, also, special thanks to Eng Hana Ebshina, Atiar Rahman, Hisham Elkhoga and Ali Assodani for their excellent support and patient for this work to be successful.

REFERENCES

[1] Petro Canda,." Geology and Petrophysics NC-177," 2005, PP35.

[2] Barr, F.T. and Weegar,A.A." Stratigraphic Nomenclatur of Sirte Basin,Libya," Petro Exploration Socisity. 1972, PP.179, 1972.

[3] M.J., Elhawat,A.S., and Sebta,A.M"Sedimentology and Hydrocarbon Potential of Gir Formation, Sirte Basin, Libya" 1996, Amsterdam, Elsevier,V.II.

[4] Sedimentary Basin of Libya First Sym COREX, " Conventional Core Analysis Study for IPLL, Well B2-NC177, 1999a.

[5] Ibrahim Musbah, Mohamed A. Elhemry, Kulud M. Rahuma, and Muhammad R. Batruna "Study of En-Naga Field Static Model Construction," Al-Azhar University Twelfth International Conference AEIC'12. Cairo, Egypt, vol. 7.No.5, pp. **529–551**, December 2012.

AUTHORS PROFILE

Dr Mohamed A.Elhemry

Department of Petroleum Engineering

University of Tripoli

Email Address: mohamedelhemry@gamil.com